LEGIBILITY NOTICE

A major purpose of the Technical Information Center is to provide the broadest dissemination possible of information contained in DOE's Research and Development Reports to business, industry, the academic community, and federal, state and local governments.

Although a small portion of this report is not reproducible, it is being made available to expedite the availability of information on the research discussed herein.

LA-UR 87-2854

CONF-8709108--10

LA-UR--87-2854

DE87 014756

Los Alamos National Laboratory is operated by the University of California for the United States Department of Energy under contract W-7405-ENG-36

TITLE: DYNAMIC PROCESSES IN FIELD-REVERSED-CONFIGURATION COMPACT TOROIDS

AUTHOR(S) D. J. REJ

SUBMITTED TO INTERNATIONAL SCHOOL OF PLASMA PHYSICS
"PIERO CALDIROLA"
VARENNA, ITALY
SEPTEMBER 1-11, 1987

DISCLAIMER

MASTER

Los Alamos Los Alamos National Laboratory
Los Alamos, New Mexico 87545

DYNAMIC PROCESSES IN FIELD-REVERSED-CONFIGURATION COMPACT TOROIDS

D. J. Rej

Los Alamos National Laboratory, Los Alamos, NM 87545, USA

ABSTRACT

In this lecture, the dynamic processes involved in field-reversed configuration (FRC) formation, translation, and compression will be revieved. Though the FRC is related to the field-reversed mirror concept, the formation method used in most experiments is a variant of the field-reversed θ-pinch. Formation of the FRC equilibrium occurs rapidly, usually in less than 20 μs. The formation sequence consists of several coupled processes: (1) preionization; (2) radial implosion and compression; (3) magnetic field line closure; (4) axial contraction; (5) equilibrium formation. Recent experiments and theory have led to a significantly improved understanding of these processes; however, the experimental method still relies on a somewhat empirical approach which involves the optimization of initial preionization plasma parameters and symmetry. New improvements in FRC formation methods include the use of lower voltages which extrapolate better to larger devices.

The axial translation of compact toroid plasmas offers an attractive engineering convenience in a fusion reactor. FRC translation has been demonstrated in several experiments worldwide, and these plasmas are found to be robust, moving at speeds up to the Alfvén velocity over distances of up to 16 m, with no degradation in the confinement.

Compact toroids are ideal for magnetic compression. Translated FRCs have been compressed and heated by imploding liners. Upcoming experiments will rely on external flux compression to heat a translated FRC at 1-GW power levels.

I. INTRODUCTION

The field-reversed configuration (FRC), a prolate compact toroid plasma without toroidal magnetic field (Fig. 1), is an attractive magnetic fusion concept because of its simple geometry, extremely large plasma beta, and natural divertor. MHD-stable FRC equilibria with impressive parameters have been created recently in modest-sized devices. For example, FRCs have been generated in the FRX-C experiment at Los Alamos with $R \leq 0.12$ m, $1\times10^{21} \leq n_e \leq 5\times10^{21}$ m^{-3}, $0.1 \leq T_i \leq 0.6$ keV, $0.1 \leq T_e \leq 0.2$ keV, $\langle\beta\rangle \approx 1$, $\tau_E \leq 100$ μs.[1] Physics issues related to FRC equilibria, stability, and transport are reviewed in companion lectures presented at this School.[2,3] In addition to these generic magnetic fusion issues, there are a number of other topics that are of special significance to the FRC and other compact toroids. In this lecture, we consider three special topics dealing with dynamic processes which can result in significant changes to the FRC: (1) formation, (2) translation, and (3) magnetic compression heating.

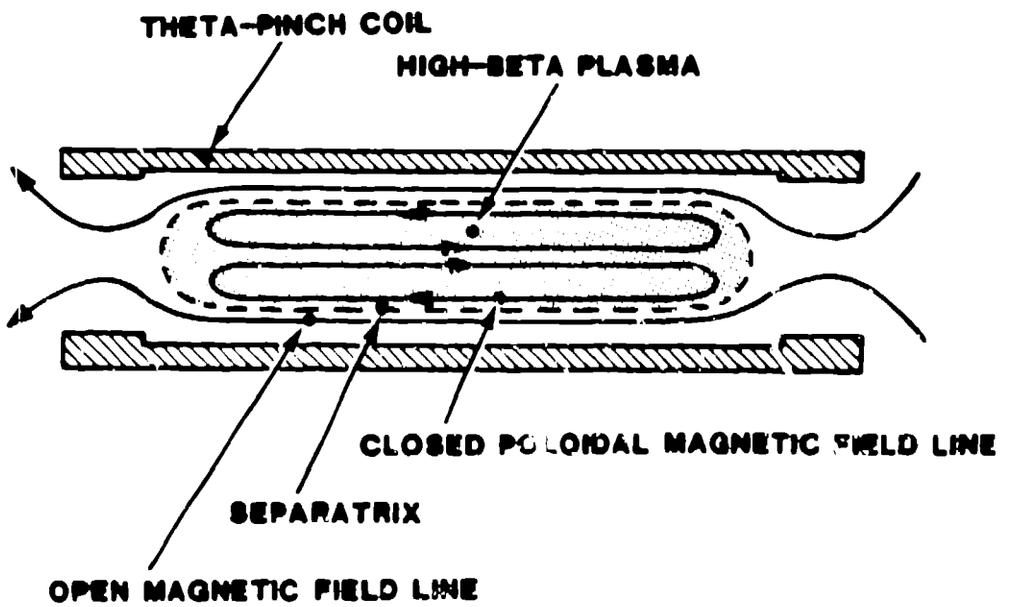

Fig. 1: The field-reversed configuration (FRC).

II. FORMATION

Though the FRC is related to the field-reversed mirror concept, the formation method used in most experiments to date is a variant of the field-reversed θ-pinch, a technique that is as old as the international

fusion program itself. Formation is a critical phase in which all of the poloidal magnetic flux and most of the plasma thermal energy is rapidly introduced to the configuration (usually in less than 20 μs) before the equilibrium is established. As discussed below the plasma configuration is highly vulnerable to destruction during this time.

The field-reversed-θ-pinch formation sequence illustrated in Figure 2 consists of several coupled processes. In a typical FRC experiment, a neutral gas (usually hydrogen or deuterium) is introduced into a cylindrical vacuum chamber mounted coaxially inside a θ-pinch coil. Both static and puff gas fill methods have been used with initial fill pressures p_o ranging between 1 and 40 mtorr. A reversed bias magnetic field B_b is then applied by discharging a capacitor bank into the θ-pinch coil. The neutral gas is subsequently preionized in the bias field (Fig. 2a). Preionization is often a two-step process. First, a low-level seed ionization is produced by use of rf, microwaves, axial currents, or oscillating multipole magnetic fields. Second, nearly full breakdown is achieved by driving internal plasma currents. The most popular techniques involve axial currents (z-pinch) driven by end electrodes and currents induced by a ringing θ-pinch or multipole. All of these preionization (PI) methods have been shown to be effective in breaking down the fill gas. On the other hand, there exists a need to improve the PI method since good plasma confinement in the FRC after formation is often linked to a quiescent, symmetric PI plasma.[1,4] It is usually difficult to experimentally obtain these optimum PI conditions. An empirical approach is normally used to establish an operational range of p_o and B_b over which an acceptable PI plasma can be produced. To date, no single PI method has clearly emerged as being superior.

After preionization, the θ-pinch coil current is rapidly reversed (Fig 2b), usually in less than a radial Alfven transit time. The PI plasma is cold with electron temperatures of several eV, but it has a sufficiently large conductivity to trap the bias flux. When the pressure from the external B-field exceeds that of the PI plasma - bias field mixture, the plasma radially implodes along with its trapped bias flux. For the configuration to be a compact toroid, the oppositely-directed B-fields must connect to one another within the vacuum vessel. Magnetic field line tearing and reconnection after the radial implosion is depicted in Fig. 2c. Until recently, this tearing-reconnection process was the standard procedure used to obtain field line closure; on

present-day experiments, auxiliary end coils are used to obtain internal field line closure without tearing during the radial implosion phase. Further elaboration about tearing and non-tearing formation is offered below. After field-line closure, an axial contraction (Fig. 2d) usually occurs since the field line tension at the ends is larger than the plasma pressure. The radial and axial shock waves eventually subside, and the plasma reaches an FRC equilibrium state (Fig. 2e).

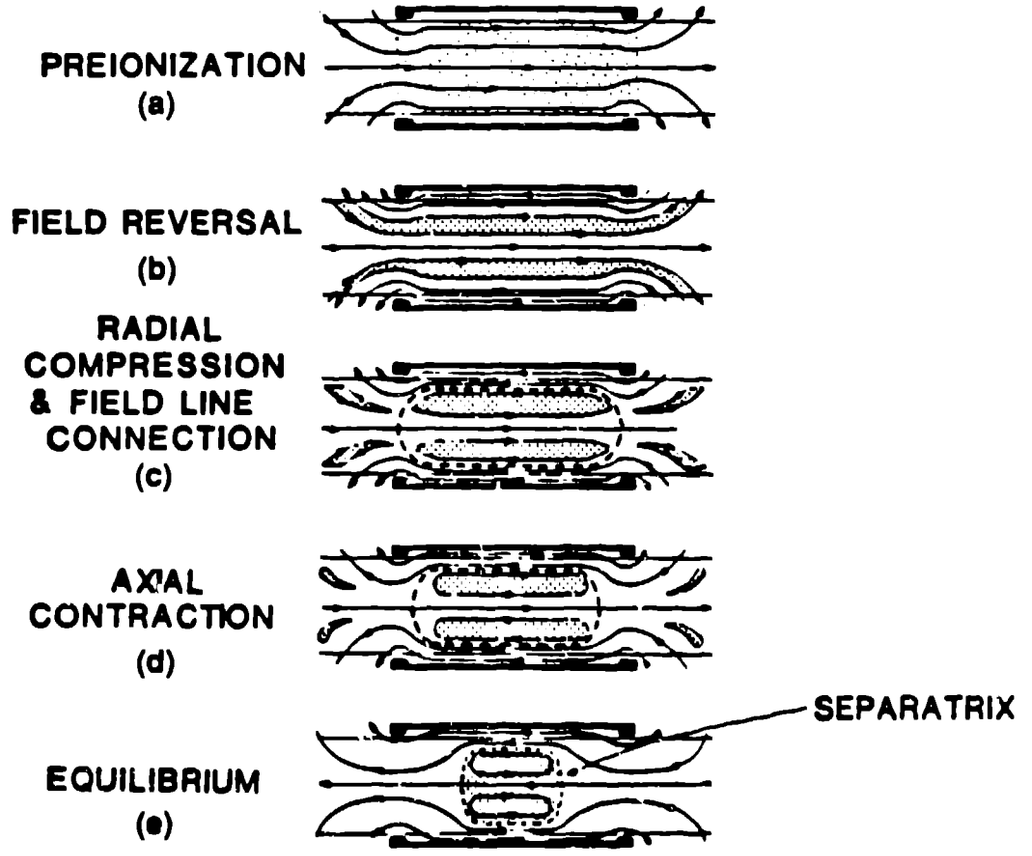

Fig. 2: The FRC formation sequence.

The FRC formation sequence is documented by the FRX-C data in Fig. 3 taken with diagnostics placed at the axial midplane.[5] Shown in this Figure are time-dependent traces of the external magnetic field B_v, the normalized diamagnetism or excluded flux $\Delta\phi$, and the integral density along a chord across the midplane. The diamagnetism is inferred using the relationship, $\Delta\phi = B_v \pi r_f^2 - \phi_l$, where ϕ_l is the magnetic flux measured by a loop placed outside the vacuum chamber at radius r_l. The reverse bias field is modulated by the θ-pinch preionization between times $-11 \lesssim t \lesssim 0$ μs. The main capacitor bank that generates the forward field

is discharged at t = 0, and field reversal occurs as B_w changes from $-B_b$ to $+B_b$. "Zero-crossing" (zc) of the field takes place at t = 0.2 μs. The forward field builds-up and when the external magnetic pressure exceeds that of the internal mixture, the plasma "lifts off" the vacuum wall and is imploded radially. The radial implosion proceeds until the first minimum in $\Delta\phi$. As B_w rises, radial oscillations in $\Delta\phi$ and $\int nd\ell$ occur from successive over and under compressions. Viscosity damps these oscillations at higher plasma temperatures. The radial compression proceeds until the maximum B_w is reached and the main capacitor bank is crowbarred.

After field line closure at the ends, the magnetic tension forces the plasma to contract axially. In Fig. 3, the plasma contracts and rebounds between times $5 \lesssim t \lesssim 9$ μs. The plasma swells radially during the contraction as evident from the increase in $\Delta\phi$. The plasma elongation (= length/diameter) decreases from an initial value of 8 to about 3 at the minimum of the axial contraction. The FRC equilibrium state is finally reached approximately 20 μs after reversal.

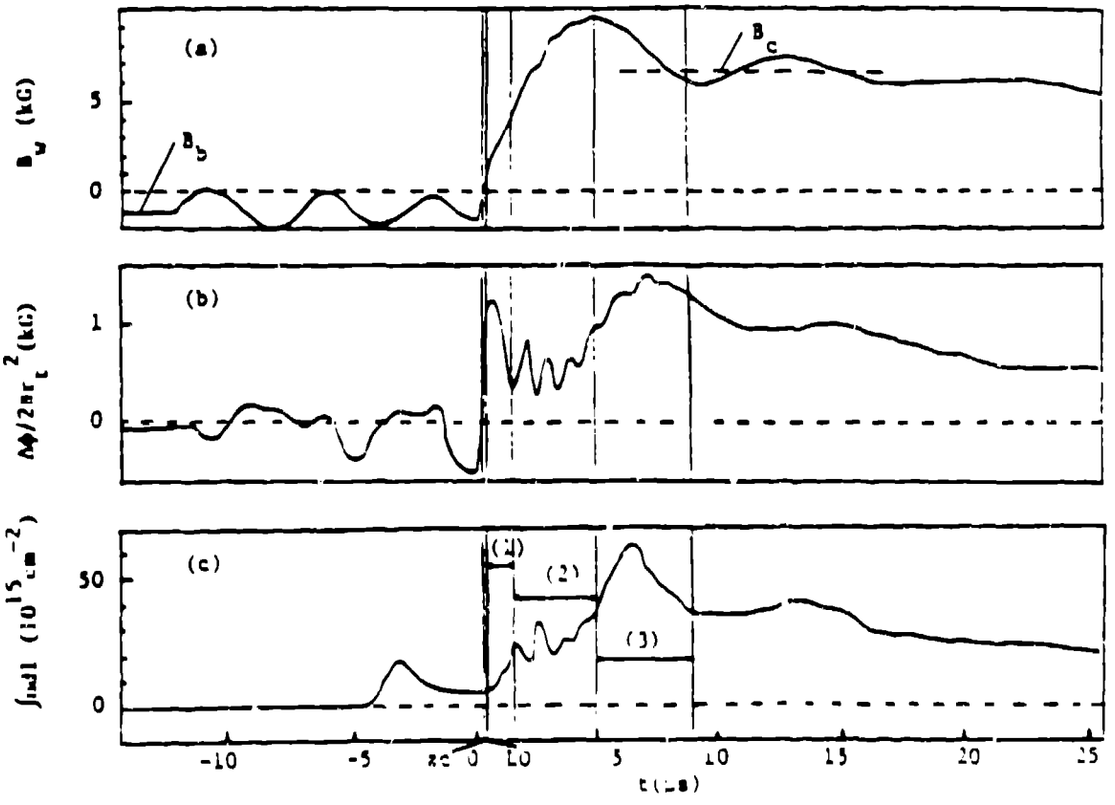

Fig. 3: FRX-C data illustrating FRC formation.

Formation with tearing reconnection is more graphically illustrated in Figure 4a by a time sequence of magnetic flux contours $\psi(r,z)$. These contours have been computed with a two-dimensional, resistive MHD code[6] for tearing-reconnection formation conditions in the FRX-C/LSM device. For simplicity, $\psi(r,z)$ surfaces are plotted over a single quadrant. Because of the assumed azimuthal symmetry, these ψ contours also can represent the magnetic field lines. Reversal of the bias field begins at time t=0. Within 2 μs after reversal, the plasma is radially imploded and the oppositely-directed field lines are connected over a region that extends beyond ends of the θ-pinch coil and the vacuum chamber wall.

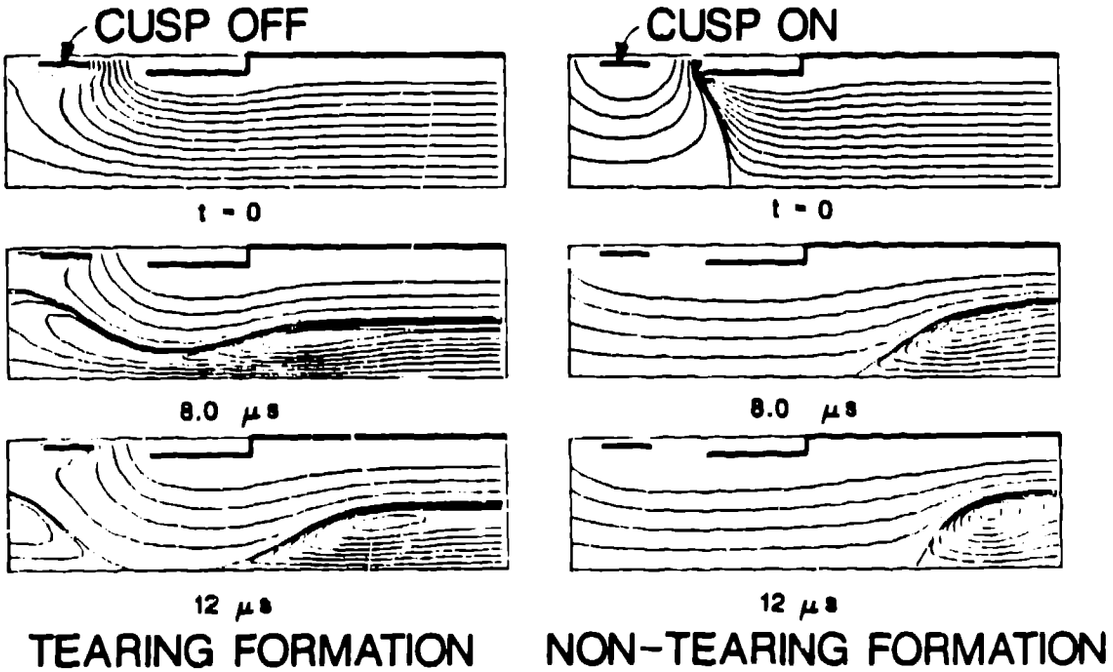

Fig. 4: MHD simulations of FRC formation on FRX-C/LSM.

Tearing reconnection occurs between times 8 and 12 μs. The severed end plasmoids are subsequently ejected out axially, carrying with them their poloidal fields, and the FRC remains inside the θ-pinch coil. Magnetic end mirrors are essential in driving tearing reconnection since they provide axial forces that rapidly evacuate plasma from under them. On FRX-C/LSM so-called "passive" mirrors are formed through a reduction in the θ-pinch coil diameter at the ends. A vacuum mirror ratio of about 1.2 is necessary on the 0.7-m-diam FRX-C/LSM θ-pinch to insure tearing reconnection. Much smaller ratios (1.1 or less) are required on smaller (0.2-m-diam) devices such as FRX-B.[7] The time of reconnection can be

controlled using the triggered reconnection technique in which the mirror fields are produced by independently-driven coils mounted at the ends of the θ-pinch.[8,9] Delaying reconnection has been used to maximize plasma heating.[8] While finite plasma resistivity η is essential for reconnection to occur, the MHD simulations indicate that the actual reconnection rate in most experiments is relatively insensitive to the resistivity magnitude. The reason for this insensitivity is the strong dynamic force under the end mirrors which evacuates some of the plasma and radially compresses the residual plasma to diameters in which resistive tearing rapidly occurs. While qualitatively predictable, tearing reconnection is by no means perfectly reproducible. Axial and azimuthal asymmetries introduced by non-uniformity in the tearing are believed to sometimes adversely affect plasma confinement. Because of these asymmetries the tearing reconnection method of FRC formation has been abandoned in recent years in favor of the non-tearing method described in the next paragraph.

The non-tearing formation method was first reported by the Kurchatov group[10] and subsequently it was extensively investigated at Spectra Technologies.[11] To achieve non-tearing formation, at least one pair of independently-driven end magnets (known as "plug" or "cusp" coils) are necessary. Non-tearing formation is illustrated in its simplest form by the MHD simulations in Fig. 4b. The end magnets are energized so that their fields are in the forward direction, thereby forming cusps with the bias field. In these simulations of the FRX-C/LSM experiment, the cusp coil current remains constant during the discharge. Internal closure of the magnetic field lines is apparent immediately following field-reversal. Any asymmetries caused by magnetic tearing are obviously avoided with this method. Indeed, direct comparison of triggered reconnection and non-tearing formation on both the TOR and TRX experiments clearly indicates that more-symmetric and reproducible FRCs are generated with the latter formation technique.[10,11] During these experiments, a second pair of driven end magnets were used. These magnets were placed between the θ-pinch and the cusps and rapidly varied at the time of reversal in order to adjust the timing of the axial contraction. Careful timing of the contraction was needed to optimize the plasma heating sequence.

In every experiment performed to date, practically all of the plasma heating occurs during formation. For example in the FRX-C/LSM device, almost all FRC thermal energy (over 20 kJ) is imparted to the plasma

during the 10 μs formation period. The plasma is heated by five processes: (1) radial implosion, (2) radial magnetic compression, (3) magnetic flux annihilation (resistive heating), (4) axial implosion, and (5) axial compression. A relatively simple but accurate FRC heating model has been developed by Steinhauer which considers these processes to occur serially.[12] Radial heating due to the implosion followed by magnetic compression is found to be substantial in present devices since the initial toroidal electric fields can range up to 1 kV/cm. The resistive or ohmic heating level depends on the amount of bias field that is annihilated during formation. An anomalous flux annihilation rate is believed to exist arising from microinstabilities driven by the steep pressure gradients present during the radial implosion. The axial shock and the resistive heating rate are coupled. The strength of the axial shock depends on the amount of trapped bias flux that is present after field line closure. As more bias flux is annihilated, the plasma pressure increases due to the increased resistive heating and the strength of the axial shock is reduced. Therefore, for a given B_b, the total energy imparted to the plasma from the resistive and axial shock heating remains relatively constant. Radial implosion heating dominates in experiments operated at low B_b and high E_θ such as on FRX-C.[1] Radial heating, while effective, has the serious drawback of requiring the use of high-voltage technologies which do not attractively extrapolate to larger-sized devices. Axial shock and resistive heating, on the other hand, become substantial in experiments at high B_b and low E_θ such as on TRX-2.[13] Operation in this regime makes more modest technological demands for larger sized machines.

As discussed by Hoffman at this School,[2] the poloidal flux ϕ_p is one of the most important FRC parameters. The critical stability and transport parameter,[2,3] $s = r_s^{-1}\int_R^r s\,(r/\rho_i)dr$ (= the average number of ion gyroradii across the minor radius of the torus), is linearly proportional to ϕ_p for fixed r_s and T_i. A challenging physics goal faced by the FRC community is to maximize ϕ_p or s in order to decrease cross-field energy losses and to check whether or not the FRC will maintain its stability against predicted MHD modes.[3] In field-reversed θ-pinch experiments, ϕ_p can never be greater than the reversed bias flux at t=0, $\phi_b = B_b(t=0)\pi r_t^2$, at the vacuum chamber wall radius r_t. In fact, a non-negligible fraction of ϕ_b is lost during formation in most experiments. For example, ϕ may be lost during field reversal, a time when the internal pressures force

the plasma and bias flux outwards, so that they contact the vacuum wall. These convective losses were first considered in 1966 by Green and Newton[14] who concluded that in order to inhibit flux loss, lift-off must occur in less than a radial Alfven time $\tau_r = r_t/v_A$. This results in a bias magnetic field limit $B_\star$, which, in practical units, is given by the formula,

$$B_\star(kG) = 1.88[E_\theta(kV/cm)]^{1/2}[A_i p_o(mtorr)]^{1/4} \quad , \qquad (1)$$

where A_i is the ion atomic mass number. Accordingly, these losses reduce the bias flux such that lift-off occurs at a reduced external field B_{LO}

$$B_{LO}/B_b = 1 - [B_b/B_\star]^2 \quad . \qquad (2)$$

Equation (2) has been confirmed experimentally on small devices operated at weak bias fields, $B_b \leq 0.5B_\star$.[15] Recent experiments and theory, on the other hand, have indicated that the Green-Newton model overestimates flux loss, especially at high bias, because of a thin, highly-conducting, pressure-bearing sheath that can form near r_t. The sheath modifies flux loss from an inertial to a slower, resistive process. Present theories[16,17] set a maximum lift-off field of approximately $2B_\star$. Fast flux annihilation could occur when operating above this limit because of increased impurity contamination arising from sheath-wall interactions. In practice, however, long-lived FRCs are produced at somewhat lower fields, $B_{LO} \leq B_\star$.[18]

We now consider the time after lift-off during which typically between 40% and 80% of the remaining flux is lost. This loss is believed to be caused by an anomalous resistivity associated with microinstabilities. Instabilities are driven by the high drift parameter associated with the steep pressure gradients that are present during compression. Little flux is lost during the axial shock because as the plasma contracts it also swells radially and pressure gradients are reduced. The most effective flux trapping during the entire formation process has been observed on the TRX-1 device where equilibrium ϕ values up to $0.3\phi_\star$ (where $\phi_\star = B_\star \pi r_t^2$) have been inferred for long-lived FRCs.[18] While the magnitude of the axial shock does not directly affect the

equilibrium flux level, it has been indirectly linked to plasma confinement properties observed afterwards. This effect is particularly evident on larger devices in which resistive heating becomes less effective and violent axial contractions can occur even at small bias fields. For example, on FRX-C/LSM, it is found that equilibrium flux confinement can deteriorate by more than an order of magnitude when there are severe axial contractions, even with non-tearing formation in a viscous regime.[5] Although the cause of this deterioration is not known at present, the axial dynamics during formation place a practical upper limit to the equilibrium flux for long-lived FRCs at a level of about $0.1\phi_*$ on FRX-C/LSM.

The field-reversed θ-pinch formation method has been proven effective in producing stable FRCs with impressive $n\tau_E$ values; however, this method has several technological and physics limitations. Implosion heating demands the use of high-voltage, high-current, pulsed-power technology (e.g., 100 kV and 3 MA on FRX-C) which becomes cumbersome when extrapolated to larger-sized machines. This technological problem will be partially circumvented on the new, 0.9-m-diameter LSX device which will operate a lower E_θ at conditions where axial shock heating, and, to a lesser extent, resistive heating are important.

Ultimately, an entirely new formation technique, one that does not necessarily couple heating and fluxing before the establishment of an equilibrium, may be desirable. Several advanced formation methods are being pursued both experimentally and theoretically. For example, initial experiments on the Coaxial Slow Source device[19] have proven successful at producing transient FRC-like plasmas at 50-times-lower E_θ than that in conventional field-reversed θ-pinches. Also, rotating magnetic fields have been effectively used to drive FRC-like geometries in modest-sized experiments.[20,21] A third method to drive FRC currents is with neutral beam injection. Exploratory beam injection start-up experiments on the 2XIIB mirror device revealed a difficulty in obtaining field-reversal because of electron counter currents.[22] This current cancellation may be avoided with multipoles[23] or with the Ohkawa effect[24] that can be enhanced when impurity ions are introduced. Indeed, experiments have been proposed to reexamine neutral beam formation or sustainment of an FRC;[25] however, no work has been performed in the laboratory since the 2XIIB experiments from a decade ago.

III. FRC TRANSLATION

Since a compact torus (CT) is not linked by materials (such as transformers, coils, and vacuum chambers), the plasma equilibrium configuration may be readily translated along its geometric axis. Translation appears to be a convenient engineering option envisioned in fusion reactors[26] since the formation, heating, and burn chamber technologies can be physically separated and the neutron wall loading may adjusted by the speed of translation. (These advantages, however, naturally compromise the linear "compactness" of the CT power plant.) FRCs have been routinely translated in several experiments worldwide.[27-29] No deterioration in confinement is observed as plasmas translate over distances of up to 16 m.[29] Besides demonstrating the translation concept, these experiments have proven important for a variety of technological and scientific reasons, for example: (1) Translation into an adjacent region with dc guide field is equivalent to application of a power crowbar. This is important since FRC lifetimes of over 300 μs are comparable to the crowbar decay time of the θ-pinch; (2) Field-reversed θ-pinch technologies (high-voltage coils, quartz vacuum chambers) are often incompatible with side-mounted, vacuum-coupled diagnostics (such as bolometry, soft x-rays, VUV spectroscopy, and internal magnetic probes). Plasma translation into a metallic vacuum chamber with low-voltage coils avoids these difficulties; (3) The s parameter can be increased by about 30% when an FRC is translated into a smaller-diameter flux conserver; (4) Every side-viewing diagnostic can observe the entire plasma length during an FRC transit past the diagnostic's field of view. Therefore, axial profiles may be inferred, given the translation speed.

A schematic drawing of the FRC translation device FRX-C/T is shown in Fig. 5. The 2-m-long field-reversing θ-pinch coil is fabricated to resemble a small-angle (1.4°) conical θ-pinch. Plasmas are accelerated by a net $j_\theta \times B_r$ force out of the θ-pinch and into a colinear translation region that is attached at the downstream end. This region consists of a 5-m-long, 0.4-m-diam metallic vacuum chamber and dc magnetic guide field B_0. A dc mirror field with magnitude up to $5B_0$ is produced at the downstream end to reflect the translating FRC.

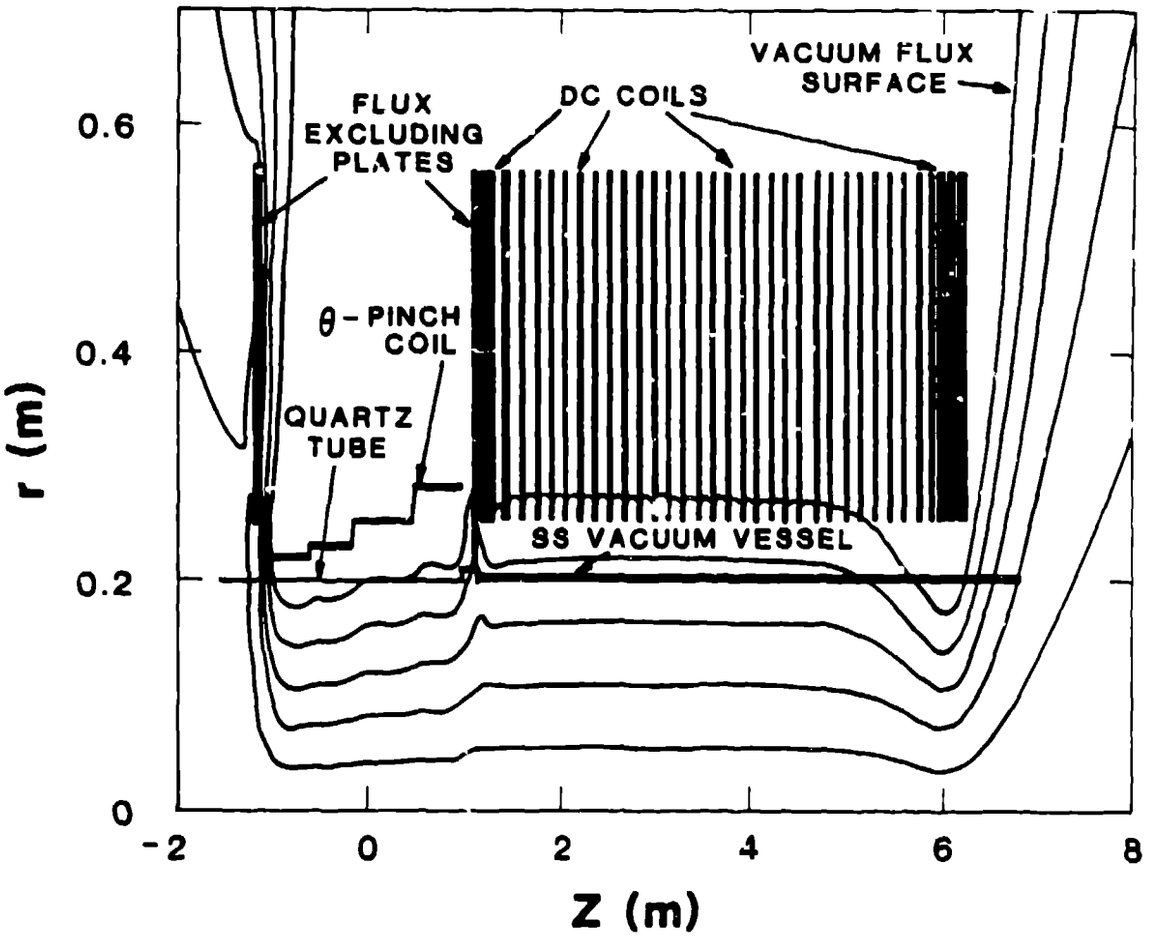

Fig. 5: Schematic drawing of the FRX-C/T experiment

FRC translation in a typical FRX-C/T discharge is illustrated by the data in Fig. 6. Plotted at approximately 18 μs intervals are the axial profiles of the plasma separatrix radius $r_s(z)$ as inferred from the measured excluded flux. The dashed line at z=0 indicates the axial midplane of the θ-pinch coil. The main capacitor bank is discharged at t=0 and the FRC is fully formed within 10 μs. Because of finite plasma inertia, the torus is not accelerated out of the θ-pinch until after FRC formation. The accelerating force on the 1-MA toroidal plasma current is about 4 kN; therefore, the characteristic acceleration time of the 2×10^{-7}kg plasma mass is of order 10 μs. Because formation and acceleration occur sequentially, there is no need for pulsed "gate" coils to initiate translation. The FRC enters the translation region (z = 115 cm) with negligible loss of E_p and ϕ_p. The FRC moves at relatively constant velocity, $v_z = 1.7\times10^5$m/s, until it is reflected by the downstream mirror. No additional losses in E_p or ϕ_p are induced by

reflection. The FRC translates back towards the source and undergoes a second reflection from the mirror formed by the crowbarred Θ-pinch coil. The plasma eventually settles down near the center of the translation region and it ultimately decays away after 200 μs.

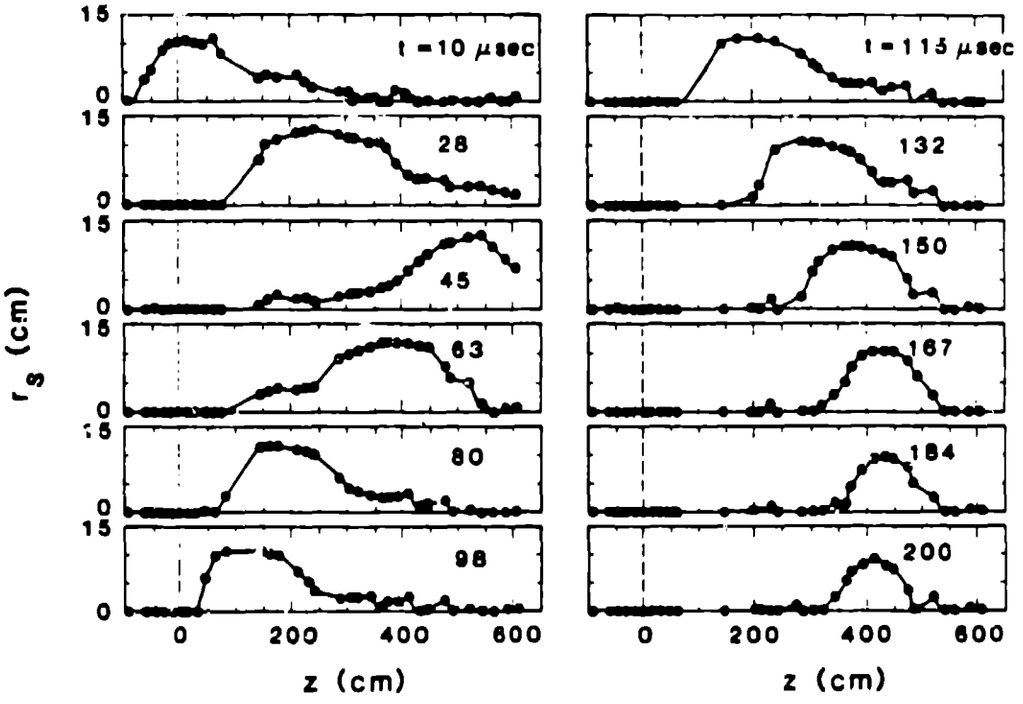

Fig. 6:
Time-evolution of the magnetic separatrix profile $r_s(z)$ of a translating FRC in a typical FRX-C/T discharge.

The translated velocity can be adjusted by the guide field strength. As B_0 is decreased, the plasma accelerates to a faster v_z at the expense of expansion cooling. Plotted in Fig. 7 are $v_z(B_0)$ data from 88 FRX-C/T discharges. Typical initial plasma parameters in the Θ-pinch were: $B_w \approx 0.6$ T, $r_s \approx 0.12$ m, $n_e \approx 1.4 \times 10^{21} m^{-3}$, and $T_e + T_i \approx 0.6$ keV. A simple model has been developed to predict v_z, given the initial plasma temperature and the vacuum magnetic field gradient. Axial kinetic energy is assumed to be gained at the expense of adiabatic magnetic decompression of the plasma and magnetic field. The model predicts v_z to lie between the two curves drawn in Fig. 7. Most of the FRX-C/T data obtained at larger guide field, $B_0 > 3$ kG, are bounded by the theory. At lower B_0, v_z appears to be limited to approximately the ion thermal speed, a value about 25% smaller than that predicted.

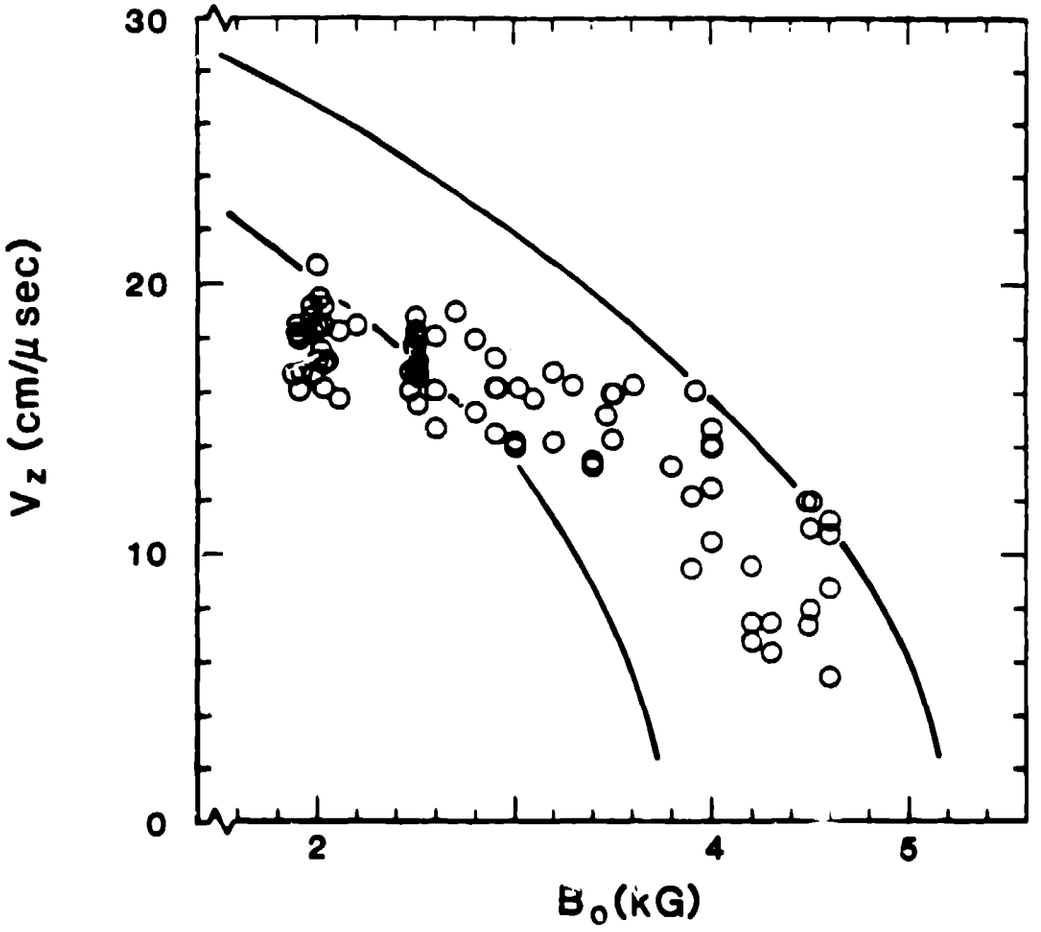

Fig. 7:
FRC translation velocity observed in FRX-C/T plotted against the applied dc guide field. Each data point is from a separate discharge.

Axial kinetic energy is lost during a reflection. As illustrated by the Fig. 8 data, the magnitude of v_z is decreased between 20 and 50%, independent of mirror ratio. The fastest moving FRCs lose the greatest amount (75%) of directed energy. This inelasticity in the reflection aids in the trapping of the FRC in the translation region. The directed kinetic energy that is lost can only sometimes be accounted for. With the largest mirror ratio, this energy appears rethermalized into the plasma; however, with smaller mirrors, this energy appears lost.

FRC translation physics is further revealed by 2-D MHD simulations of the FRX-C/T data (Fig. 9). Field line closure is asymmetric; tearing reconnection occurs under the upstream mirror while the cusp formed between the bias and the dc guide field insure non-tearing closure downstream. The MHD code quantitatively predicts the behavior shown by

the Fig. 6 data, including the axial kinetic energy losses during a reflection; however, the computation indicates that this energy is rethermalized into the plasma, an effect that is not always observed experimentally. The simulations also indicate that the translation dynamics can distort the plasma configuration far away from equilibrium.

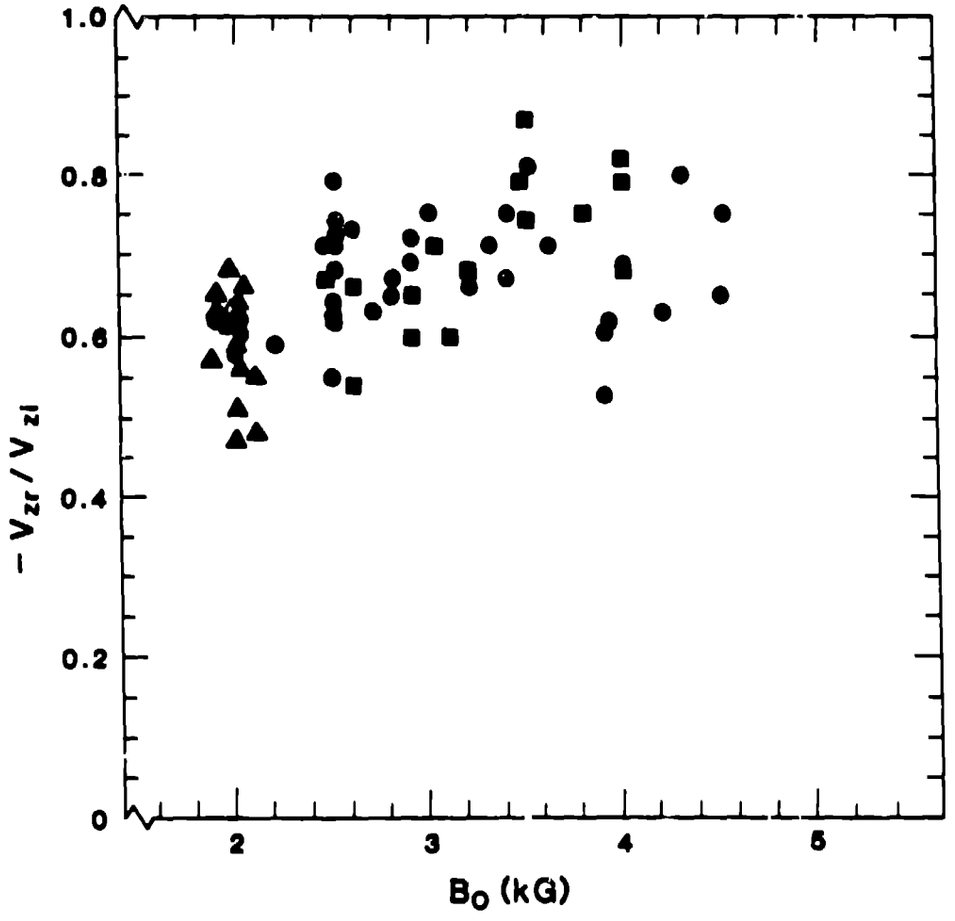

Fig. 8:
Ratio of FRC translation velocity after to before reflection from end mirror plotted against the applied dc guide field.

This fact is illustrated in Fig. 10 in which the domain of $p(\psi)$, computed over the entire 2-dimensional simulation grid, is plotted for three times corresponding to the middle of the first transit, the reflection, and the middle of the second transit through the translation region. In view of the large range of $p(\psi)$ during the reflection, one must conclude that an FRC is a robust object that can endure significant perturbations away from equilibrium without deterioration in confinement.

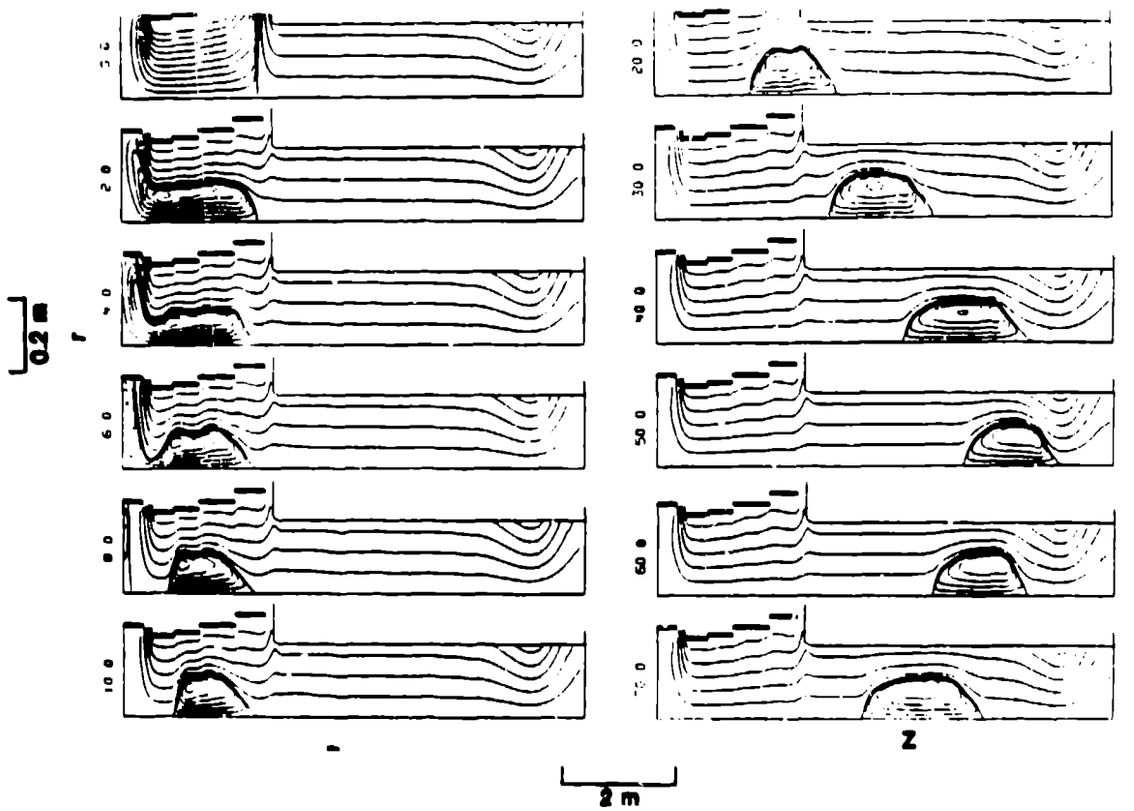

Fig. 9: Two-dimensional MHD simulations of FRC translation in FRX-C/T.

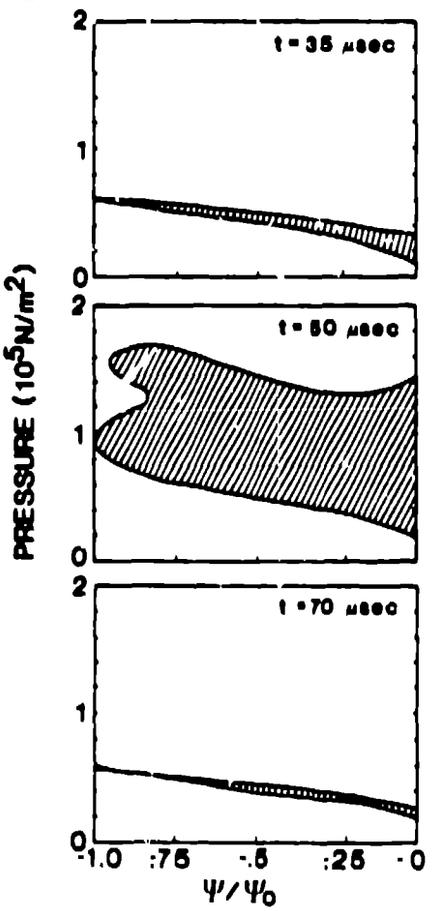

Fig. 10: Calculated domain of plasma pressures plotted as a function of the poloidal flux Ψ for the same MHD simulation as is shown in Fig. 9. Flux is normalized to that at the magnetic axis.

IV. HIGH-POWER MAGNETIC COMPRESSION HEATING

As discussed in §II, most of the heating in practically every FRC experiment occurs during formation. Auxiliary heating of the equilibrium plasma represents an important new step in FRC research since it would extend parameter space to higher temperatures. In particular, a heating experiment should allow better understanding of confinement issues such as the observed anomalous cross-field electron thermal conductivity, particle convection rate, and field-null resistivity.

Because of the relatively high-energy density (or β) and short confinement times observed in present FRC plasmas, an auxiliary heating experiment will demand extraordinary power levels. For example, the FRX-C/LSM plasma contains about 20 kJ of thermal energy that is confined up to 100 μs; therefore, input power levels of order 1 GW will be required in order to offset the 200 MW losses and heat the FRC. Magnetic compression is particularly attractive as an auxiliary heating method because of its low cost, relative efficiency (especially when coupled with plasma translation), and proven reliability. The physics of adiabatic magnetic compression is well understood, being verified on tokamaks,[30] mirrors[31] and field-reversing electron rings.[32]

The only high-power, FRC compression heating experiment to date have been the wall compression studies performed on the TL device,[27] in which a shaped liner was imploded around a translated FRC. The observed neutron yield (2×10^8) indicated substantial ion heating. Zero-dimensional modeling of these results imply a volume compression ratio of up to 6000 and T_i values of at least 1.5 keV.[33]

In late 1988, the FRX-C/LSM device will be modified in order to permit high-power magnetic compression studies. The external flux outside a translated FRC will be increased four-fold. Flux compression is preferred over liner compression because of its greater simplicity, compatibility with plasma diagnostics, and the higher repetition rate.

A conceptual design of the FRX-C magnetic compression experiment is shown in Fig. 11. The device will be divided into three stages: (1) the FRX-C/LSM field-reversed θ-pinch source in which the FRC will be formed and launched; (2) a central compression region; (3) a confinement stage, consisting primarily of the FRX-C/T translation region, in which the translated, compressed FRC will be trapped. The formation and confinement stage hardware already exist and the design of the 4-m-long, 0.5-m-diameter compressor is now underway.

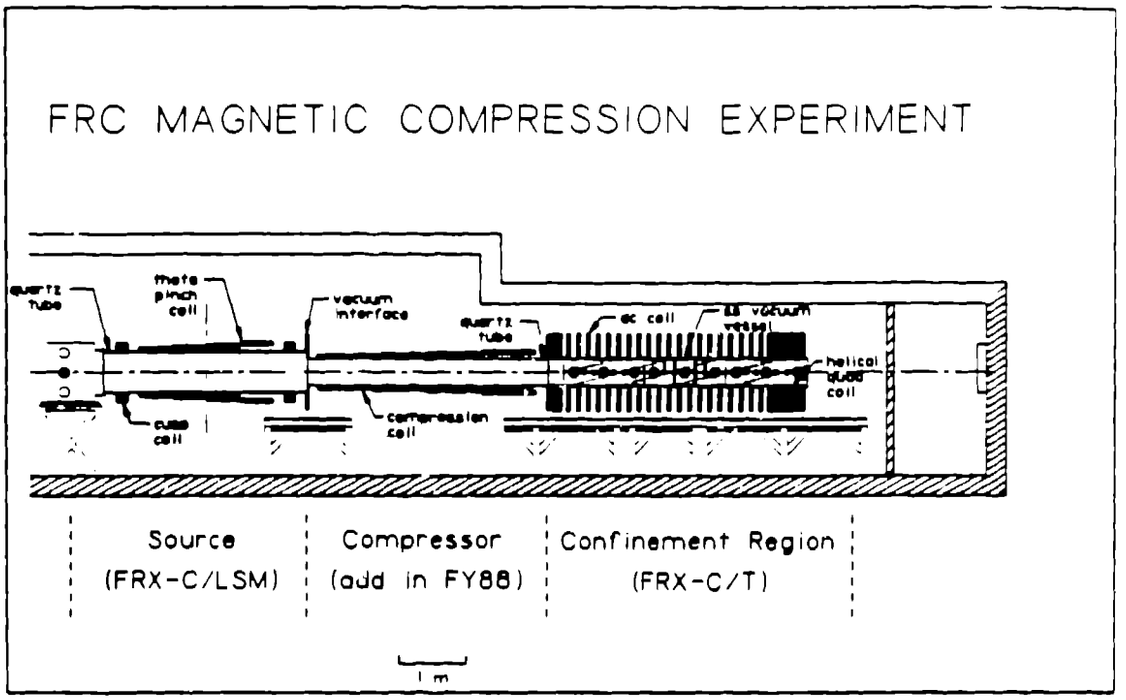

Fig. 11: Conceptual drawing of the FRX-C magnetic compression experiment.

Adiabatic compression theory[34] predicts a substantial increase in plasma energy on FRX-C (60 kJ or more). A zero-dimensional transport model[35,36] indicates substantial improvements in plasma parameters from adiabatic compressional heating even when anomalous diffusion is included. The sample transport simulations illustrated in Fig. 12 are based on optimized initial conditions presently obtained on FRX-C/LSM: $\bar{n} = 1\times10^{21}m^{-3}$, $T_e+T_i = 0.6$ keV, $r_s = 0.18$ m, separatrix length $\ell_s = 1.6$ m, $\phi_p = 6$ mWb, $s = 2$. The FRC is translated into the compressor at times, $10 \leq t \leq 20$ μs, with the wall radius and external flux reduced in a manner that is compatible with translation energetics.[37] Magnetic compression occurs between times $40 < t < 70$ μs. The external B-field is increased from about 0.5 T to over 2 T, and the plasma is compressed with r_s and ℓ_s decreasing from 0.15 to 0.09 m and 2.8 to 1.0 m, respectively. The final plasma density and temperatures depend on the transport physics. Convection and conduction losses caused by the lower-hybrid-drift (LHD) instability[38] do not appreciably change the final parameters from those obtained in the no-loss case: $n = 6\times10^{21}m^{-3}$ and $T_e+T_i = 1.8$ keV. Poloidal flux loss in this simulation is computed for a typical diffuse profile equilibrium with a field-null resistivity equal to 8 times the classical perpendicular value. The simulation

indicates a substantial increase in the confinement parameter, $n\tau_E \approx 6\times10^{17}$ s m^{-3} at $T_i \approx 1$ keV. On the other hand, if the cross-field electron thermal conductivity $\kappa_\perp$ becomes even more anomalous (as illustrated by the simulation in Fig. 12 where $\kappa_\perp$ predicted by a microtearing instability theory[39] is used), the electron temperature could remain clamped well-below 0.5 keV; consequently, the ions will cool because of the faster equilibration with electrons. The anomalous electron losses in this calculation force the energy to decay faster than ϕ_p. These fast losses result in an axial contraction which is responsible for the plasma density increase to over 10^{22}m^{-3}.

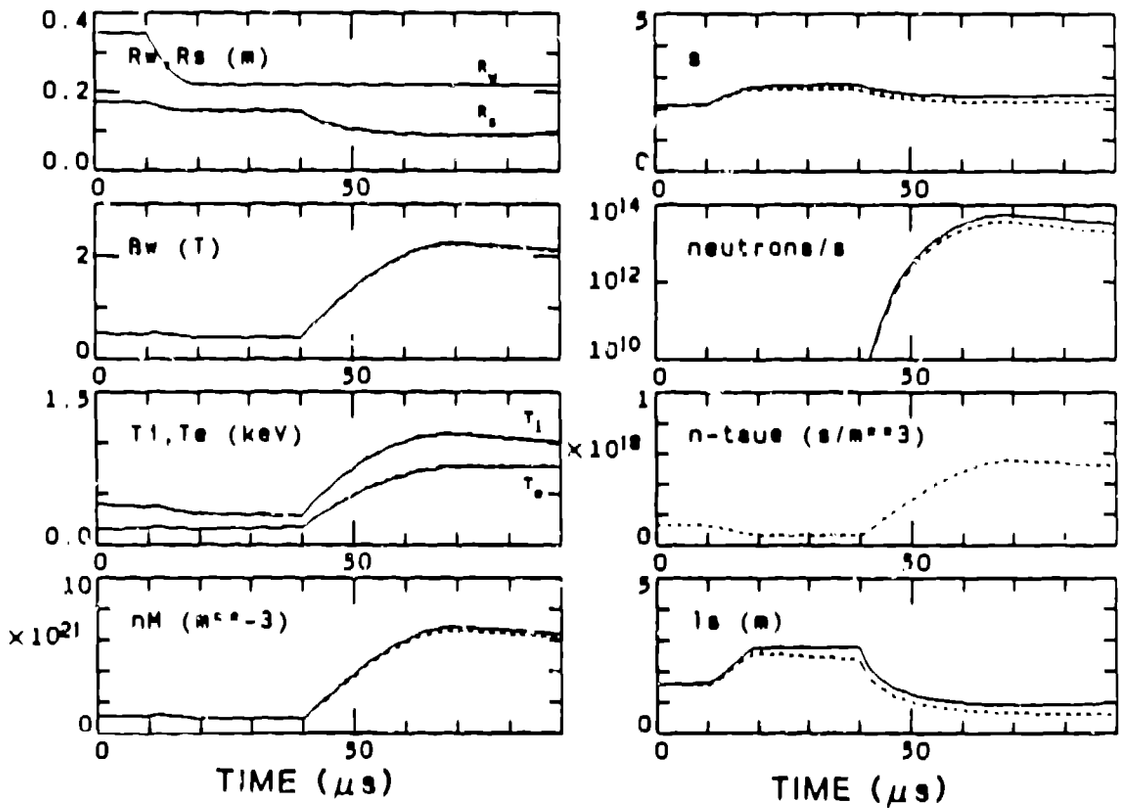

Fig. 12:
Zero-dimensional simulations of magnetic compression heating of translated FRX-C/LSM plasmas. The three simulations correspond to (1) no-losses (solid-lines); LHD particle convection and thermal conduction and eight-times classical poloidal flux decay (dashed lines); (3) anomalous electron thermal conduction from the microtearing mode in addition to the losses considered in case 2 (dotted lines).

ACKNOWLEDGMENTS

Technical discussions with members of the Los Alamos compact torus groups are gratefully acknowledged. The author is particularly indebted to Dr. M. Tuszewski for much of the material presented in §II. FRC research at Los Alamos is funded by the U.S. Department of Energy.

REFERENCES

/1/ R. E. Siemon et al., Fusion Technology 9, 13 (1986).
/2/ A. L. Hoffman, these proceedings.
/3/ D. C. Barnes, these proceedings.
/4/ L. C. Steinhauer et al., Phys. Fluids 28, 888 (1985).
/5/ M. Tuszewski, to be published.
/6/ R. D. Milroy, J. U. Brackbill, Phys. Fluids 25, 775 (1982).
/7/ W. T. Armstrong et al., Phys. Fluids 24, 2068 (1981).
/8/ A. G. Es'kov et al., Plasma Physics and Controlled Nuclear Fusion Research 1978 (IAEA, Vienna, 1979) II, 187.
/9/ W. T. Armstrong et al., Phys. Fluids 24, 2121 (1982).
/10/ V. V. Belikov et al., Plasma Physics and Controlled Nuclear Fusion Research 1982 (IAEA, Vienna, 1983) II, 343.
/11/ J. T. Slough et al., Nuclear Fusion 24, 1537 (1984).
/12/ L. C. Steinhauer, Phys. Fluids 26, 254 (1983).
/13/ A. L. Hoffman and J. T. Slough, Nuclear Fusion 26, 1693 (1986).
/14/ T. S. Green and A. A. Newton, Phys. Fluids 9, 1386 (1966).
/15/ S. O. Knox et al., Phys. Fluids 25, 362 (1982).
/16/ M. I. Kutuzov et al., Sov. J. Plasma Phys. 7, 520 (1981).
/17/ R. D. Milroy et al., Phys. Fluids 27, 1545 (1984).
/18/ A. L. Hoffman et al., Fusion Technology 9, 48 (1986).
/19/ Z. A. Pietrzyk et al., Nuclear Fusion (in press).
/20/ H. Tuczek, private communication.
/21/ I. R. Jones, A. Knight, Proc. 12th European Conf. on Contr. Fusion and Plasma Physics (EPS, Budapest, 1985), I, 647.
/22/ W. C. Turner et al., Nuclear Fusion 19, 1011 (1979).
/23/ J. H. Hammer, H. L. Berk, Nuclear Fusion 22, 89 (1982).
/24/ D. Baldwin et al., Comments Plasma Phys Contr. Fus. 4, 55 (1978).
/25/ K Hirano, Nucl Fus. 24, 1159 (1984), & Nagoya Rep IPPJ-827 (1987).
/26/ e.g., R. Hagenson, R. Krakowski, in Fusion Reactor Design and Technology (IAEA, Vienna. 1983), I, 377.
/27/ S. G. Alikhanov et al., Op cit. Ref. 10, III, 319.
/28/ M. Tanjyo et al., Plasma Physics and Controlled Nuclear Fusion Research 1984 (IAEA, Vienna, 1985) II, 523.
/29/ D. J. Rej et al., Phys. Fluids 29, 852 (1986).
/30/ Plasmas have been adiabatically compressed in the ATC, TFTR, TOSCA, and TUMAN-IIA tokamaks.
/31/ e.g., F. Coensgen et al., Phys. Fluids 9, 187 (1966).
/32/ M. Tuszewski et al., Phys. Rev. Lett. 43, 449 (1979).
/33/ A. G. Es'kov et al., Sov. Tech. Phys. Lett. 9, 16 (1983).
/34/ R. Spencer et al., Phys. Fluids 26, 1564 (1983).
/35/ D. J. Rej, M. Tuszewski, Phys. Fluids 27, 1514 (1984).
/36/ M. Tuszewski et al., Phys. Fluids 29, 863 (1986).
/37/ R. E. Chrien, Phys. Fluids 28, 3426 (1985).
/38/ M. Tuszewski, R. K. Linford, Phys. Fluids 25, 765 (1982).
/39/ J. Drake et al., Phys. Rev. Lett. 44, 994 (1980).